

Properties of a Once-Broken Wormlike Chain Based on Amylose Tricarbanilate. Light Scattering, Viscosity, and Dielectric Relaxation[†]

Beate Pfannemüller,* Manfred Schmidt,* and Gerd Ziegast

Institute of Macromolecular Chemistry, University of Freiburg, D-7800 Freiburg i.Br., Federal Republic of Germany

Keizo Matsuo

*Technical-Chemical Laboratory, ETH-Center, CH-8092 Zürich, Switzerland.
Received August 1, 1983*

ABSTRACT: The paper deals with a new type of A-B-A polymer which is composed of two amylose tricarbanilate chains of equal length (A) connected by a flexible joint (B) consisting of a polymethylene or poly(ethylene oxide) chain of variable length. The products are obtained by a combined chemical and enzymatic reaction, i.e., coupling of maltooligomers onto both ends of a diamino derivative of B via an amide linkage and subsequent use of the maltooligomeric stubs as primers for the enzymatic chain elongation. This procedure leads to almost monodisperse amylose chains ($P_w/P_n < 1.005$) of any desired length. Depending on mono- or bifunctional maltooligomeric primers, the corresponding A and A-B-A polymers may be produced. Light scattering, viscosity, and dielectric relaxation measurements of the tricarbanilyl derivatives in dioxane revealed that within experimental error the flexible spacer B did not affect the geometric and hydrodynamic dimensions of the A-B-A samples as compared to those of the pure A polymers. The Kuhn length of both the A and the A-B-A samples was determined to $180 \leq \lambda^{-1} \leq 260$ Å, depending on the applied experimental method. An independent proof for the existence of the A-B-A-type molecules was obtained by the dielectric relaxation behavior: the A and the A-B-A samples exhibited a completely different molecular weight dependence of the dielectric loss peak frequency as could be expected theoretically for head-to-tail and head-to-head structures, respectively.

Introduction

In 1984 we will have the 100th anniversary of Werner Kuhn's birthday. He is the pioneering scientist who first introduced the idea of the random coil into polymer chemistry,¹ a concept which has proved immensely fruitful in the past. Hermann Staudinger, on the other hand, was for a long time strongly convinced of the rodlike nature of linear macromolecules in solution.² The whole polymer science has since developed between these poles. Just after the war, Kratky and Porod³ created the wormlike chain, which is called the limiting continuous chain in the fundamental mathematical framework by Daniels.⁴ The wormlike chain has attracted the interest of Walter H. Stockmayer for a long time. He invented the intermediate structures of the broken chain⁵ and the once-broken rod.⁶ Here we wish to introduce another modification of chain structures between the two extremes mentioned above, i.e., the once-broken worm. According to the theoretical work of Stockmayer and co-workers, the difference in the solution properties of the perfect and the once-broken rod is expected to be small.⁶ Although we are aware of this fact, we still found it interesting to see by experiment whether there is a difference between a wormlike and a once-broken wormlike chain.

The tricarbanilate derivative of amylose has been the subject of extensive investigation.⁷⁻¹³ From early light scattering and viscosity measurements in different solvents Burchard and Husemann^{7,8} determined exponents of 0.90-0.92 in the Mark-Houwink equation, indicating a considerable chain stiffness. A helical structure stabilized by hydrogen bonds between adjacent substituents was first proposed by Bittiger and Keilich¹⁴ from circular dichroism studies in dioxane. Among the various helix conformations suggested in those days, a wormlike fourfold helix with a pitch height of 10.4 Å was found to best fit the experi-

mental data for the chain length dependence of the mean square radius of gyration.¹² According to recent X-ray fiber studies by Zugenmaier,¹⁵ the preferred conformation of amylose derivatives is probably a four- to fivefold helix.

This paper deals with a new type of A-B-A polymer, which is composed of two amylose tricarbanilate chains (A) connected by a flexible joint (B) consisting of a short polymethylene or poly(ethylene oxide) chain. These molecules are obtained by a combined chemical and enzymatic reaction. In a first step maltooligomers (A) carrying an aldono-lactone end group are coupled onto both ends of a diamino derivative of the B component via an amide linkage.¹⁶⁻¹⁸ The short maltooligomeric stubs are subsequently used as primers for further enzymatic chain elongation, leading to amylose sequences of almost any desired length. The kinetics of the phosphorolytic synthesis are analogous to those of the living anionic polymerization, producing a narrow molecular weight distribution ($P_w/P_n \leq 1.005$).^{19,20} The length of the amylose branches can easily be regulated by the primer concentration. Depending on mono- or bifunctional maltooligomeric primers, the corresponding A and A-B-A polymers may be obtained covering a wide range of molecular weight.

Since amylose tricarbanilate is regarded as a stiff or wormlike polymer, the goal of our investigation was to determine whether an influence of the flexible joints B and their sequence length on the geometric and hydrodynamic molecular dimensions of the samples can be observed. To the best of our knowledge, this is the first work of this kind dealing with "once-broken wormlike chains", named analogously to the "once-broken rod" created by Yu and Stockmayer.⁶

Experimental Section

A. Sample Preparation. Uniform Amylose Tricarbanilates (A). Amyloses were enzymatically synthesized from glucose 1-phosphate with potato phosphorylase, using different amounts of maltotetraose as primer. (The chain length is determined by

[†]This once-broken worm is affectionately dedicated to Professor Walter H. Stockmayer on the occasion of his 70th birthday.

the mole ratio of monomer to primer.^{21,22}) The tricarbanilyl derivatives were prepared by reaction of amylose with phenyl isocyanate in pyridine.^{7,23}

Once-Broken Amylose Tricarbanilates (A-B-A). Pure maltooligomers with a degree of polymerization of 6 or 7 obtained by gel permeation chromatography on Bio-Gel P2 or P4 were converted to their aldonic acid lactones by electrolytic oxidation,²⁴ treatment with cation-exchange resin, and evaporation.²⁵ Coupling of the aldonic acid lactone to a difunctional carrier with amino end groups (B) via an amide linkage was carried out in ethylene glycol at 70 °C.¹⁷ The B components were (i) oligo(methylene-diamines), $H_2N-(CH_2)_n-NH_2$ ($n = 2, 6$, and 12), (ii) oligo(ethylene oxide) with amino end groups, i.e., $H_2N-CH_2CH_2-(OCH_2CH_2)_5-NH_2$,¹⁸ and (iii) an α,ω -diamino derivative of poly(ethylene oxide) (PEO). The latter product was prepared from PEO 2000 (Merck) by reaction of the ditosyl ester with the potassium salt of 2-aminoethanethiol, an improved modification of the method by Kern et al.^{26,27} Purification of the A-B-A samples, i.e., removal of unreacted aldonic acid lactones and monosubstituted product (A-B), was achieved by chromatographic separation on Bio-Gel P4 or P10 containing a small proportion of carboxylic groups (introduced by saponification of a few acrylamide bonds), thus taking advantage of both the molecular sieve effect of the gel and the ion-exchange properties.²⁷ All A-B-A primers were readily soluble in water, a necessary condition for the subsequent enzymatic chain elongation to narrow molecular weight amylose chains. Phosphoryl syntheses were carried out as described before.^{21,22} By varying the primer concentration, a series of products covering a wide range of molecular weights was prepared from each type of bifunctional primers. The tricarbanilate derivatives were prepared as described above.

All solvents used for the preparation of the samples and for the physical measurements were purified according to the standard procedures.

B. Physical Measurements. Viscosity Measurements. The viscosity measurements were performed in dioxane with an Ostwald viscosimeter. The influence of the shear gradient on the intrinsic viscosity of the high molecular weight samples (above $M_w \sim 10^6$) was determined with a special Ubbelohde viscosimeter as described elsewhere.⁷

Light Scattering Measurements. Static or frequency-integrated light scattering (ILS) and dynamic or quasi-elastic light scattering (QLS) measurements were performed with a Malvern K7023 96-channel correlator which allows the simultaneous recording of the scattering intensity and of the time correlation function (TCF).²⁸ A krypton ion laser (Spectra Physics, Model 164-11) operating at 647.1-nm wavelength was used as the light source. The samples were dissolved in dioxane at least 24 h prior to the measurement. The concentration ranged from 1.2–3.0 mg/mL for the smallest molecular weight to 0.2–1.2 mg/mL for the highest molecular weight. The solutions were clarified with a Beckman ultracentrifuge L50 with a swinging-bucket rotor (Model SW 25.1), applying a special floating technique with cesium chloride as the density agent.²⁹ The centrifugation time varied according to the molecular weight from 1.0 to 2.5 h at 15 000 rpm.

Data Analysis. The TCF was analyzed according to the method of cumulants:

$$\ln g_1(t) = -\Gamma t + \frac{1}{2}\mu_2(\Gamma t)^2 - \frac{1}{6}\mu_3(\Gamma t)^3 \quad (1)$$

with $\Gamma \equiv -(d \ln g_1(t)/dt)_{t \rightarrow 0}$. Γ is called the first cumulant, $\mu_2 \equiv \Gamma_2/\Gamma^2$ and $\mu_3 \equiv \Gamma_3/\Gamma^3$ are measures of the deviation from a single-exponential decay. Extrapolated to zero angle, the reduced first cumulant Γ/q^2 yields the z-average translational diffusion coefficient, $\lim_{q \rightarrow 0} (\Gamma/q^2) = D_z$, where $q = (4\pi/\lambda) \sin(\theta/2)$, with θ the scattering angle and λ the wavelength of the scattered light in the medium. In all cases a second-order fit with respect to t described the time correlation function satisfactorily and the third-order fit did not improve the variance significantly. For all samples the sample time τ was selected to fulfill the condition $\Gamma t_{\max} = \Gamma \tau n_{\max} \geq 5$, with n_{\max} the last time channel in the correlator. Although our correlator is equipped with 96 time channels only, for the present measurements n_{\max} equals 348, because a delay of 256 τ occurs after the first 80 channels (four channels are lost for this delay); the last 12 channels from 336 τ to 348 τ are used to monitor the base line. The ILS data were plotted as suggested by Zimm,³⁰ which allows the evaluation of the

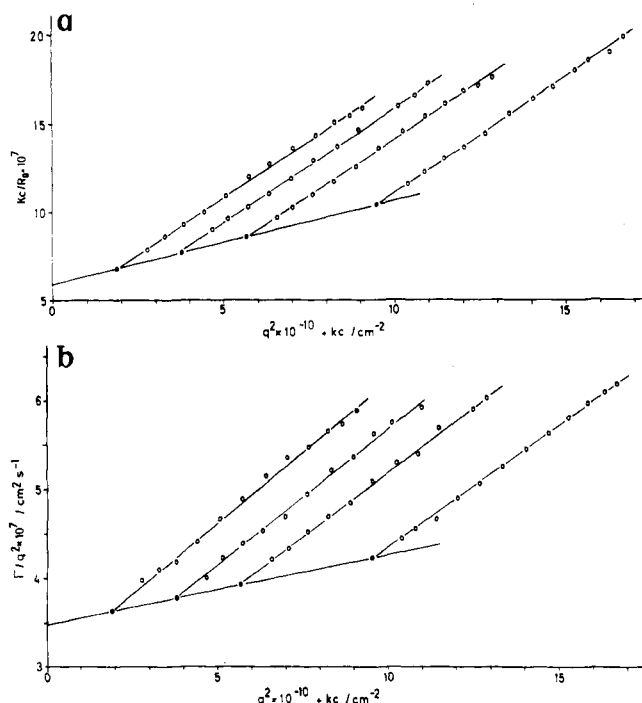


Figure 1. Static (a) and dynamic (b) Zimm plot of amylose tricarbanilate ($M_w = 1.7 \times 10^6$).

weight-average molecular weight, M_w , of the z-average mean square radius of gyration, $\langle S^2 \rangle_z$, and the second virial coefficient A_2 . A similar plot was proposed²⁸ for the reduced first cumulant where Γ/q^2 replaces the reduced scattering intensity Kc/R_90 in the original Zimm plot. One example of Zimm plots of simultaneously measured ILS and QLS data is given in Figure 1.

The "dynamic" Zimm plot (b) yields the infinite-dilution diffusion coefficient D_z when the concentration and the magnitude of the scattering vector approach zero; in the analogous "static" Zimm plot (a) M_w is obtained. The slope of the q^2 dependence, when extrapolated to zero concentration, yields $C\langle S^2 \rangle_z$, where C is a structure-dependent dimensionless quantity.^{31,32} The slope of the concentration dependence for $q \rightarrow 0$ gives $k_D D_z$, where k_D is the coefficient of the concentration-dependent translational diffusion coefficient according to

$$D_z(c) = D_z(0)(1 + k_D c) \quad (2)$$

Dielectric Measurements. Capacitances and conductances were measured for dilute solutions (1.3–1.8 mg/mL) of polymers in freshly distilled dioxane at 40 different frequencies between 10 and 10^5 Hz with a General Radio 1621 precision capacitance measurement system installed at the Electrotechnique Center of the Swiss Federal Institute of Technology, Zürich. The home-built dielectric cell with a three-terminal method requires 4.2 mL of solution. The capacitor within the cell, consisting of four concentric stainless steel cylindrical plates without spacers in solution, had a vacuum capacitance of 9.143 pF. Temperature was controlled by immersing the cell into a water bath regulated at 25 ± 0.03 °C. Capacitances and conductances were determined to ± 0.002 pF and ± 0.1 p Ω^{-1} , respectively. The dielectric constant and the loss factor were obtained in the same way as described before.^{33,34}

Results and Discussion

The uniform A and the A-B-A samples were characterized by static and dynamic light scattering, by viscosity, and by dielectric relaxation measurements. The results are listed in Table I.

Light Scattering. The molecular weight dependence of the radius of gyration, $\langle S^2 \rangle_z^{1/2}$, and of the hydrodynamic radius R_h ($R_h = kT/6\pi\eta_0 D_z$) is shown in Figure 2 for the A and for the A-B-A polymers. In spite of the flexible joint in the A-B-A triblock copolymers the geometric and hydrodynamic dimensions of these block copolymers are

Table I
Results from Static and Dynamic Light Scattering, Viscosity, and Dielectric Relaxation

product	$M_w \times 10^{-5}$	P_w	$L_w,^a$ nm	$\langle S^2 \rangle_z^{1/2},$ nm	$R_h,$ nm	$A_2 \times 10^4,$ $\text{cm}^3 \cdot \text{mol}^{-1} \cdot \text{g}^{-2}$	$k_D,$ $\text{cm}^3 \cdot \text{g}^{-1}$	k_{f0}^b	C	$[\eta],$ $\text{cm}^3 \cdot \text{g}^{-1}$	$f_{\text{max}},$ kHz
A-B-A ^c	1.61	310	114.8							56.1	56.00
A-B-A ^d	2.00	385	142.6	23.0	13.0	3.62	20.5	4.56		78.0	36.00
A	2.06	397	146.8	22.0	13.7	3.41	24.0	3.70		86.5	11.00
A	2.91	560 ^f	207.2							97.6	8.90
A-B-A ^c	3.53	680	251.6	31.8	17.6	3.00	20.5			128.8	
A-B-A ^d	3.94	760	281.2	34.6		3.60				144.0	10.20
A	5.40	1040	385.0	43.0	22.5	2.50	45.1	4.22		132.5	
A	8.53	1643	608.0	58.0	32.0	1.60	35.0	2.45	0.18 ± 0.01	297.0	
A	12.00	2300 ^f	851.0							366.0	0.44
A-B-A ^d	13.00	2505	926.8	66.5	42.2	2.15	148.0	2.81	0.15 ± 0.01	385.0	1.10
A	17.00	3276	1212.0	83.5	49.0	2.45	198.0	3.64	0.14 ± 0.01	462.5	0.24
A	29.00	5600 ^f	2072.0							835.0	0.085
A-B-A ^e	31.10	6000 ^f	2220.0							885.0	0.19
A-B-A ^d	33.00	6350	2349.5	126.0	74.5	1.70				995.0	0.18

^a $h = 3.7 \text{ \AA}$. ^b According to eq 4-6. ^c $B = -(\text{CH}_2)_{12}-$. ^d $B = -(\text{CH}_2)_6-$. ^e $B = -(\text{CH}_2\text{CH}_2\text{O})_6-$. ^f M_w determined from the molecular weight dependence of the intrinsic viscosity (see Figure 3).

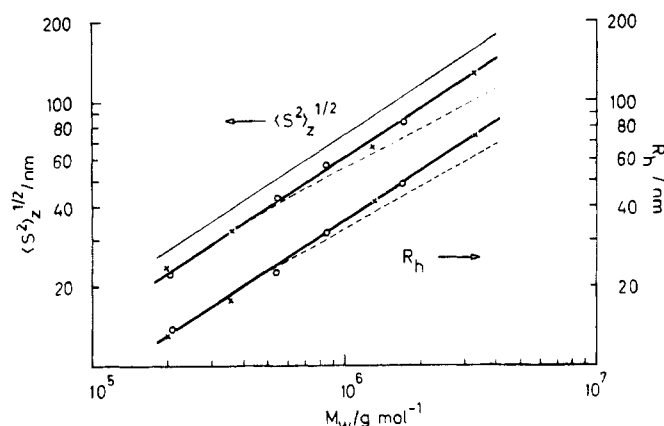


Figure 2. Molecular weight dependence of the radius of gyration (upper curves) and of the hydrodynamic radius (lower curves) for A-B-A (X) and A (O) type amylose tricarbanilates in dioxane. The dashed lines are calculated by employing $\lambda^{-1} = 260 \text{ \AA}$, $h = 3.7 \text{ \AA}$, and $d = 20 \text{ \AA}$. The full curve on top represents earlier measurements by Burchard.¹⁰

apparently the same as for the pure A homopolymers.

Next we tried to analyze the chain stiffness of the amylose tricarbanilates in dioxane from the ILS and QLS data on the basis of the wormlike chain model of Kratky and Porod.³ The radius of gyration was first calculated by Benoit and Doty³⁵ as

$$\langle S^2 \rangle = \frac{L}{6\lambda} - \frac{1}{4\lambda^2} + \frac{1}{4\lambda^3 L} - \frac{1}{8\lambda^4 L^2} (1 - \exp(-2\lambda L)) \quad (3)$$

with L the length measured along the contour of the chain and λ^{-1} the Kuhn statistical length.

In recent years the hydrodynamic radius for a Kratky-Porod chain was calculated by employing various approximations for the moments of the segment distribution function.^{5,36,37} Here we have used the Koyama theory³⁸ for the segment distribution, and we calculated some values by numerical integration.

As indicated in Figure 2 the experimental data of the molecular weight dependence of $\langle S^2 \rangle_z^{1/2}$ can hardly be described by the theoretical relation given by eq 3. Qualitatively the same discrepancy between experiment and theory is found for R_h as may be recognized from Figure 2. For both calculations a contour length $L_w = P_w h$ was taken, with P_w the weight-average degree of polymerization and h the "contour" length per monomer residue, where h is the pitch height of a helix divided by the

number of units per turn. A value of $h = 3.7 \text{ \AA}$ in the calculation of L_w was chosen, which was obtained by X-ray investigations of Zugenmaier and Gutknecht³⁹ on a similar amylose derivative, tribenzoyl amylose. This value may be slightly different in a rather wobbled helix of the amylose tricarbanilate in solution. The theoretical calculation of R_h requires besides the contour length the hydrodynamically effective cross section d of the polymer chain, which for the amylose tricarbanilate is of the order of 20 \AA .¹²

Dioxane is a good solvent for amylose tricarbanilate and it appears therefore likely that the difference between the experimental and the theoretical curves results from a growing influence of the excluded volume with increasing chain length. This argument is qualitatively supported by the fact that the deviation of the experimental data from the theoretical curve is significantly larger for the radius of gyration than for R_h . For the lower molecular weights the excluded volume effect is, of course, almost negligible. This statement holds true especially for stiff chains since the ring-closure probability approaches zero at $\lambda L < 10$.⁴⁰ Thus we may conclude that a theoretical fit with only the three lowest molecular weights will yield a statistical segment length close to that of the unperturbed chain. We now find a value of $\lambda^{-1} = 260 \text{ \AA}$, which is smaller than $\lambda^{-1} = 310 \text{ \AA}$ reported by Burchard¹² but higher than $\lambda^{-1} = 206 \text{ \AA}$ obtained by Brant and co-workers⁴¹ by the analysis of Burchard's data with an improved theory. Moreover, Burchard has employed a value of $h = 4.025 \text{ \AA}$ based on a fourfold helix. With $h = 3.7 \text{ \AA}$ used in the present work the Kuhn length derived from Burchard's data would increase to $\lambda^{-1} = 340 \text{ \AA}$. The difference from our value of $\lambda^{-1} = 260 \text{ \AA}$ results mainly from the fact that our recent ILS measurements give about 15% smaller radii of gyration than determined earlier by Burchard¹⁰ in dioxane (see Figure 2).⁴²

Dimensionless Quantity C . The quantity C evaluated from the angular dependence of the reduced first cumulant, λ/q^2 , is included in Table I. These values are significantly lower than calculated by Schmidt and Stockmayer.³⁷ This deviation is attributed to the limited time resolution of the correlator, which does not measure the zero-time value, $C(t = 0) \equiv C$, but rather a quantity $C(t)$.⁴³ $C(t)$ becomes smaller as t increases and eventually decays to zero for $t \rightarrow \infty$.

Concentration Dependence of D_2 . The second virial coefficient, A_2 , and the concentration dependence, k_D , of the diffusion coefficient are related to the concentration

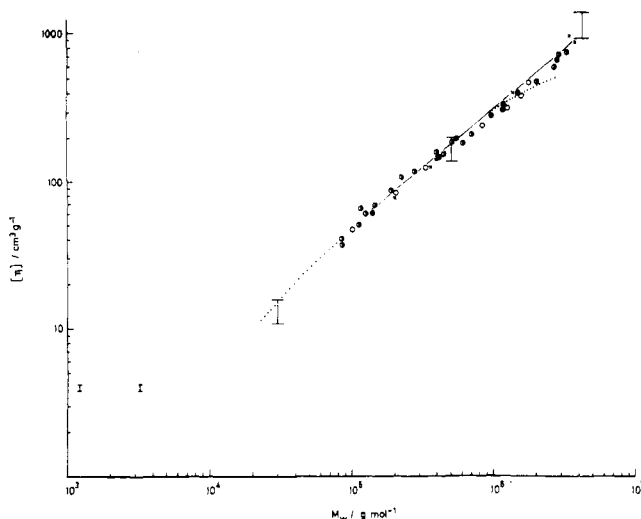


Figure 3. Molecular weight dependence of the viscosity number for A-B-A (×), A (○), and mixtures (●) of A and A-B-A polymers. The error bars stand for earlier measurements by Sutter and Burchard.¹³ The dotted curve is calculated with $\lambda^{-1} = 180 \text{ Å}$, $h = 3.7 \text{ Å}$, and $d = 20 \text{ Å}$.

dependence of k_f of the friction coefficient, $f, f(c) = f(0)(1 + k_f c)$ by⁴⁰

$$k_f + k_D = 2A_2M - \bar{v}_2 \quad (4)$$

with \bar{v} the partial specific volume of the polymer. Various theoretical calculations of k_f agree insofar⁴⁵⁻⁴⁷ that

$$k_f = k_{f0} N_L V_h / M \quad (5)$$

N_L stands for Avogadro's number, k_{f0} has the meaning of an interpenetration parameter, which has been evaluated theoretically for some models as discussed later, and V_h is the hydrodynamic volume, which may be expressed as

$$V_h = 4\pi R_h^3 / 3 \quad (6)$$

Inserting the experimental values of A_2 , k_D , M_w , and R_h into 4-6, we evaluated the parameter k_{f0} as listed in Table I. According to Pyun and Fixman,⁴⁵ $k_{f0} = 2.23$ for a soft-sphere model simulating a flexible coil in a Θ solvent and $k_{f0} = 7.16$ for a hard-sphere model simulating a flexible polymer in a good solvent. The latter value has been modified by calculations of Batchelor⁴⁸ and Felderhof⁴⁹ to $k_{f0} = 6.66$ and by Akcasu⁵⁰ to $k_{f0} = 6.00$. (A detailed discussion of the problem is given by Felderhof.⁴⁹)

The influence of chain stiffness on k_{f0} is not yet known theoretically. Experimentally, we notice two facts: (i) the k_{f0} values for amylose tricarbanilate are smaller than those for flexible polymers in a good solvent but not as low as in Θ solvents. (ii) As the molecular weight decreases, i.e., when the chain becomes more rodlike since λL decreases, an increase of k_{f0} is observed; this is in qualitative agreement with a recent investigation of poly(benzyl glutamate) in a helicogenic solvent.⁵¹

Viscosity. As could be anticipated from the light scattering results the molecular weight dependence of the limiting viscosity number gives no indication for an increased flexibility of the A-B-A polymers as compared to the A homopolymers (Figure 3). Within the experimental error, our viscosity data agree with former measurements,^{7,8,13} although our data lie a little below (molecular weight higher than 1.2×10^6) and above (molecular weight smaller than 5×10^5) the least-squares-fitted calibration curve of Sutter and Burchard.¹³ (The range of scattering data from these studies is marked in Figure 3.) This finding gave rise to a slight shift in the viscosity-molecular weight relationship, which is shown in Figure 3 as the full line.

Many attempts have been made^{44,52,53} to evaluate the intrinsic viscosity of a wormlike chain in terms of structural parameters, with unsatisfactory results so far. Still, one always has to introduce the approximation of "preaveraged hydrodynamics" in order to make the theoretical equations mathematically tractable.⁴⁴ Nonetheless we adopted the dynamical model of Harris and Hearst,⁵² which is formally equivalent to the Zimm model⁵⁴ for flexible chains but includes bending motions as the chain gets stiffer. The viscosity was derived by following the procedure of Zimm for flexible chains, with the result

$$[\eta] = 2\pi N_L (\lambda L)^3 / (\lambda^2 M_L) \sum_{i=1}^N (\gamma_i L^4) \quad (7)$$

where N_L is Avogadro's number, M_L the mass per unit length, λ^{-1} the Kuhn statistical length, and $\gamma_i L^4$ the non-draining eigenvalues as evaluated by Hearst, Beals, and Harris.⁵³ Hydrodynamic interaction between the polymer segments is included. With the aid of eq 7 we tried to fit the experimental viscosity data over the whole molecular weight region employing the same values for h and d as given in the light scattering section. No reasonable fit of the experimental data could be achieved. Following the same arguments as for the interpretation of the light scattering results, we then fitted the theoretical curve only to the smallest molecular weights, i.e., $M_w \leq 5 \times 10^5$. Accordingly, the dotted curve in Figure 3 was obtained, which corresponds to a Kuhn length of $\lambda^{-1} = 180 \text{ Å}$. The deviation of the experimental data from this curve at higher molecular weights is interpreted as the effect of an increasing influence of excluded volume. The value of $\lambda^{-1} = 180 \text{ Å}$ is considerably lower than $\lambda^{-1} = 260 \text{ Å}$ determined by light scattering but fairly close to the value of $\lambda^{-1} = 206 \text{ Å}$ obtained by Brant and co-workers.⁴¹ The deviation of λ^{-1} from that of the light scattering result is beyond experimental error but might be due to deficiencies in the viscosity theory either in the dynamical model itself or, as we tend to believe, in the "preaverage" approximation of the Oseen hydrodynamic interaction of the polymer segments.

Dielectric Relaxation Measurements. In 1957 Scherer et al.⁵⁵ observed that cellulose derivatives exhibit a low-frequency dielectric loss peak, with the peak frequency, f_{\max} , strongly dependent on the molecular weight of the samples. At much higher frequencies another, molecular weight independent, loss peak occurred, which has been attributed to the relaxation of the dipoles in the side chains being uncorrelated with the long-range motions of the polymer backbone. First measurements on amylose tricarbanilates reported by Gupta et al.⁵⁶ also investigated the low- and the high-frequency absorptions.

The present study is confined to the low-frequency loss peak, which results from the relaxation of the dipole components directed along the contour of the polymer backbone. Since the relaxation of the dipole moment components along the polymer backbone reflects the segmental motion of the chain, the maximum dielectric loss frequency is related to the relaxation times of the polymer segments as described by the spring-and-bead model.^{54,57,58} For monomeric units of a polymer chain, i.e., dipole moments of a monomer unit which are linked together head-to-tail, the dielectric loss peak frequency, f_{\max} , is caused by all odd normal modes, as was shown by Stockmayer and Baur.³⁴ The net dipole moment vanishes for every even mode. Thus, the chief contribution to the dielectric spectrum comes from the first normal mode

$$1/(2\pi f_{\max}) = 2\tau_1 \quad (8a)$$

with τ_n the "viscosity" relaxation times, which are half the

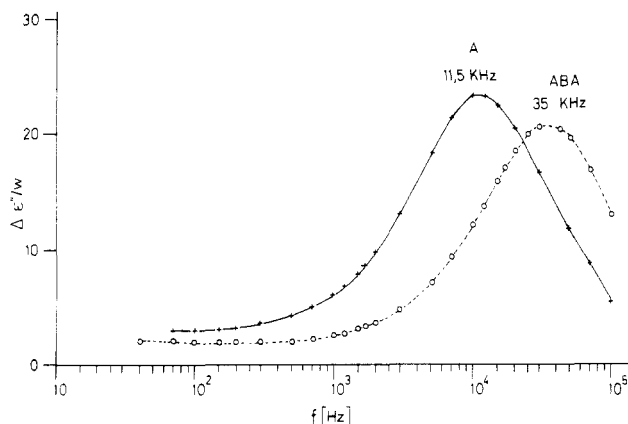


Figure 4. Dielectric loss as a function of frequency for an A-B-A ($P_w = 385$) and an A ($P_w = 395$) sample.

dielectric relaxation times of the n th mode, and N the number of segments of the polymer. For two head-to-tail chains coupled head-to-head, the dipole moment of all odd and of every other even, i.e., $4n$ th ($n = 1, 2, \dots$), mode vanishes and the peak frequency arises essentially from the second normal mode

$$1/(2\pi f_{\max}) = 2\tau_2 \quad (8b)$$

Since the relaxation time decreases strongly with the number n of the normal mode, a significant shift of f_{\max} should be observed from the head-to-tail chain to the head-to-head polymer of the same total molecular weight. Such a difference in f_{\max} is indeed observed for the A and A-B-A polymers as shown for a pair of samples in Figure 4. The shift of the dielectric loss peak clearly indicates the different behavior of the A and A-B-A chains.

The molecular weight dependence of f_{\max} may be interpreted in terms of the normal mode relaxation times. Since the relaxation times can be expected to vary with the chain stiffness, we again adopted the Harris-Hearst model to extract information about the chain stiffness from the molecular weight dependence of f_{\max} for the A and A-B-A chains, respectively. According to Harris and Hearst⁵² the relaxation times are given by

$$\tau_k = \frac{\eta_0}{kT} (2\pi\lambda^{-3})(\lambda L)^4 (\gamma_k L^4)^{-1} \quad (9)$$

with kT the thermal energy, η_0 the solvent viscosity, and $\gamma_k L^4$ again the nondraining eigenvalues of Hearst, Beals, and Harris.⁵³ Inserting eq 9 into (8a) and (8b), one obtains for the A homopolymer

$$\frac{1}{2\pi f_{\max}} = \frac{\eta_0}{kT} (4\pi\lambda^{-3})(\lambda L)^4 (\gamma_1 L^4)^{-1} \quad (10a)$$

and for the A-B-A structure

$$\frac{1}{2\pi f_{\max}} = \frac{\eta_0}{kT} (4\pi\lambda^{-3})(\lambda L)^4 (\gamma_2 L^4)^{-1} \quad (10b)$$

Figure 5 shows the data of the experimentally measured quantity $(kT/\eta_0)(1/2\pi f_{\max})$ and the theoretical curves plotted as a function of M_w . For comparison the experimental data of the pure A chain reported by Gupta et al.⁵⁶ are included in Figure 5. Since the degree of polymerization, P_w , of these samples has been determined by viscosity measurements using the calibration curve of Sutter and Burchard,¹³ we reevaluated P_w of these samples from the full-line curve in Figure 3. The revised data (solid circles) are in good agreement with our measurements. The best fit of the experimental data of the A homopolymers to the low molecular weights was obtained with $\lambda^{-1} = 180$ Å. At larger chain lengths deviations occur again,

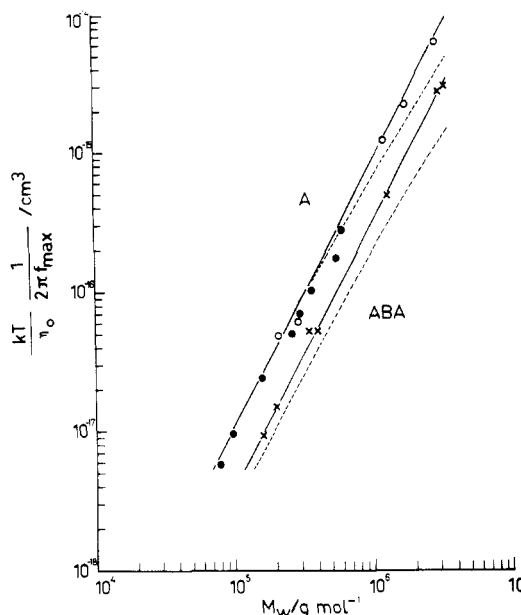


Figure 5. Molecular weight dependence of the reduced dielectric loss peak frequency: (X) A-B-A; (O) A; (●) A (taken from ref 56). The dashed curves are calculated according to eq 10a for the A polymers and eq 10b for the A-B-A polymers, respectively, with $\lambda^{-1} = 180$ Å, $h = 3.7$ Å, and $d = 20$ Å.

which are attributed to the excluded volume as discussed earlier. The value $\lambda^{-1} = 180$ Å is identical with the viscosity result. This agreement is not surprising, because both quantities, viscosity and f_{\max} , are related through the rotational diffusion coefficient and were calculated by the same dynamical model and the same eigenvalues and relaxation times. The lower dashed curve in Figure 5 was calculated for the A-B-A samples, assuming as for the fit of the A polymer $\lambda^{-1} = 180$ Å. Evidently, this curve does not exactly describe the experimental data.

Unfortunately, this deviation cannot be explained by an increased chain flexibility of the A-B-A structure. Such an effect would cause an even larger difference between the experimental values and the theoretical calculation instead of the observed assimilation. It seems not meaningful to attribute a higher chain stiffness to the A-B-A than to the A polymers. It should be noted that the theoretical curve for the A-B-A structure is only valid if the internal modes of motion are not at all disturbed or damped by the more flexible B block. The little higher experimental data might indicate that the internal motions of the A blocks are a bit out of phase, thus allowing a small contribution of the odd modes. There are other possibilities to explain the discrepancy. As indicated by HPLC some A-B-A samples contain a small amount (less than 10%) of pure A polymer of roughly half the molecular weight. Such a contamination of A polymer causes the dielectric loss peak to shift to lower frequencies. However, an estimation of this effect shows that a 25–30% content of A polymer would be needed to explain the deviation. This point and a possibly asymmetric A_x-B-A_y structure⁵⁹ need further studies in order to allow a more detailed discussion.

Conclusions

The present investigation reveals a still not fully clarified picture concerning the chain stiffness of the amylose tri-carbanilate chains in dioxane. Light scattering measurements in a θ solvent by Burchard¹² and the results from dielectric measurements by Gupta et al.⁵⁶ gave a Kuhn length in the range of $\lambda^{-1} = 300$ Å. The combined ILS and QLS measurements lead to a Kuhn length of $\lambda^{-1} = 260$ Å,

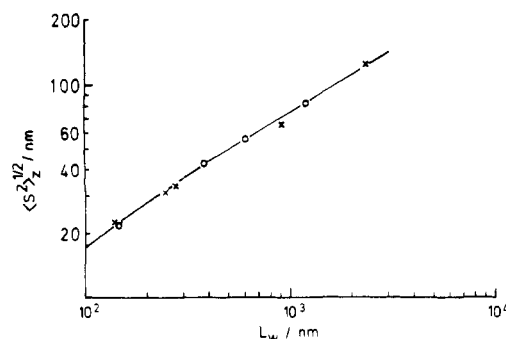


Figure 6. Molecular weight dependence of the radius of gyration with symbols as in Figure 2. The solid curve represents the theoretical calculation according to eq 11 with $\epsilon = 0.1$ and $\lambda^{-1} = 260 \text{ \AA}$.

which is in good agreement with the earlier studies. The viscosity data and our new dielectric relaxation measurements favor on the contrary an even smaller Kuhn length of $\lambda^{-1} = 180 \text{ \AA}$. The difference may be attributed to the hydrodynamic preaverage approximation involved in the calculation of the eigenvalues by Hearst, Beals, and Harris.⁵³ The interpretation of the light scattering results is somewhat ambiguous, since the influence of the excluded volume could only be estimated. However, the Kuhn length of the "unperturbed state" of amylose tricarbanilates is smaller than 260 \AA , if the smallest molecular weights are still expanded due to the good solvent. This is in agreement with the reevaluation of the older data¹² by the recent theory by Brant et al.⁴¹ These authors considered the possibility that long-range cooperative interactions of the carbanilate side chains might cause the chain stiffness to increase as the molecular weight increases. The calculations showed that the cooperativity in amylose tricarbanilates has reached its asymptotic value at a degree of polymerization of 80, far below our range of investigation. These calculations lead to a theoretical Kuhn length of $\lambda^{-1} = 210 \text{ \AA}$, not too far from our experimental results.

Coming back to the main reason for the study of these molecules, we can state that the flexible joint in a wormlike chain of moderate stiffness has no detectable effect on the common static and dynamic properties of the chain, which are measured by static and dynamic light scattering and by viscosity. However, when the directional property of an electric dipole is taken into consideration, then the head-to-head coupled nature of the A-B-A chain becomes clearly recognizable and allows an unambiguous differentiation of such block copolymers from pure A blocks. This point leads us to the question of the physical nature of the joint B. There can be no doubt that the helical structure of the A-B-A-type amylose tricarbanilate is interrupted. In this respect the introduction of a nonhelical B block mimics a break in the supermolecular structure. Such a break is obviously not capable of changing the overall flexibility of the polymer significantly, even if the length of the B block is increased from six to twelve methylene groups or when methylene groups are replaced by ethylene oxide repeating units (see Table I). The dielectric measurements, however, reveal that the B block may slightly perturb the correlation of the segmental motions between the two A chains. In our opinion the dielectric relaxation measurements present the most exciting result of the present study.

Added Note. One of the referees of this paper drew our attention to the papers of Sharp and Bloomfield,^{60,61} which take account of the excluded volume effect on the dimensions of wormlike chains. The first Daniel's distri-

bution function⁴ has been modified and leads for the mean square radius of gyration to

$$\langle S^2 \rangle = \frac{\lambda^{\epsilon-1} L^{\epsilon+1}}{(\epsilon+2)(\epsilon+3)} \left\{ 1 - \frac{\epsilon+3}{2\lambda L(\epsilon+1)} \right\} \quad (11)$$

with ϵ the excluded volume parameter as introduced by Bloomfield and Zimm.⁶²

We tried to fit our experimental data with this relationship leaving $\lambda^{-1} = 260 \text{ \AA}$ and varying only ϵ . As shown in Figure 6 a good fit is obtained with $\epsilon = 0.1$.

Acknowledgment. Our collaboration originates from our common personal relationship with Professor W. H. Stockmayer. We all thank him as a mentor and as a friend. We are greatly indebted to Professor W. Burchard for many suggestions and stimulating discussions. M.S. thanks Professor J. E. Hearst, who kindly provided us with unpublished nondraining eigenvalues of the Harris-Hearst model. K.M. thanks Mr. Neiger at the Electrotechnique Center, ETH Zürich, for allowing him to use the capacitance bridge. This work was supported by the Deutsche Forschungsgemeinschaft (B.P., G.Z., and M.S.) and by the Forschungsfond of the Eidgenössische Technische Hochschule, ETH-Center, Zürich (K.M.).

Registry No. Amylose tricarbanilate, 9047-05-6.

References and Notes

- (1) Kuhn, W. *Angew. Chem.* **1936**, *49*, 858; **1938**, *51*, 640.
- (2) Staudinger, H. In "Fortschritte der Chemie, Physik und Technik der makromolekularen Stoffe"; Röhrs, W., Staudinger, H., Vieweg, R. Eds.; J. F. Lehmanns Verlag: München/Berlin, 1939; pp 1-27.
- (3) Kratky, O.; Porod, G. *Recl. Trav. Chim. Pays-Bas* **1949**, *68*, 1106.
- (4) Daniels, H. E. *Proc. R. Soc. Edinburgh, Sect. A* **1952**, *63*, 290.
- (5) Hearst, J. E.; Stockmayer, W. H. *J. Chem. Phys.* **1962**, *37*, 1425.
- (6) Yu, H.; Stockmayer, W. H. *J. Chem. Phys.* **1967**, *47*, 1369.
- (7) Burchard, W.; Husemann, E. *Makromol. Chem.* **1961**, *44-46*, 358.
- (8) Husemann, E.; Burchard, W.; Pfannemüller, B.; Werner, R. *Stärke* **1961**, *13*, 196.
- (9) Burchard, W. *Z. Phys. Chem. (Frankfurt/Main)* **1964**, *42*, 293.
- (10) Burchard, W. *Makromol. Chem.* **1965**, *88*, 11.
- (11) Burchard, W. *Chem. Soc., Spec. Publ.* **1969**, *23*, 135.
- (12) Burchard, W. *Br. Polym. J.* **1971**, *3*, 214.
- (13) Sutter, W.; Burchard, W. *Makromol. Chem.* **1978**, *179*, 1961.
- (14) Bittiger, H.; Keilich, G. *Biopolymers* **1969**, *7*, 539.
- (15) Zugenmaier, P. Personal communication at the European Science Foundation Workshop on "Specific Interactions in Polysaccharide Systems", Uppsala, 1983.
- (16) Emmerling, W. N.; Pfannemüller, B. *Makromol. Chem.* **1978**, *179*, 1627.
- (17) Emmerling, W. N.; Pfannemüller, B. *Starch/Stärke* **1981**, *33*, 202.
- (18) Ziegast, G.; Pfannemüller, B. *Polym. Bull.* **1981**, *4*, 467.
- (19) Pfannemüller, B.; Burchard, W. *Makromol. Chem.* **1969**, *121*, 1.
- (20) Pfannemüller, B. *Naturwissenschaften* **1975**, *62*, 231.
- (21) Husemann, E.; Pfannemüller, B. *Makromol. Chem.* **1963**, *69*, 74.
- (22) Pfannemüller, B. *Stärke* **1968**, *20*, 351.
- (23) Husemann, E.; Pfannemüller, B. *Makromol. Chem.* **1961**, *49*, 214.
- (24) Isbell, H. S.; Frush, H. L. *Methods Carbohydr. Chem.* **1963**, *2*, 14.
- (25) Emmerling, W. N.; Pfannemüller, B. *Carbohydr. Res.* **1980**, *86*, 321.
- (26) Kern, W.; Iwabuchi, S.; Sato, H.; Böhmer, V. *Makromol. Chem.* **1979**, *180*, 2539.
- (27) Ziegast, G.; Pfannemüller, B. *Makromol. Chem.*, submitted.
- (28) Bantle, S.; Schmidt, M.; Burchard, W. *Macromolecules* **1982**, *15*, 1604.
- (29) Dandliker, W. B.; Kraut, J. *J. Am. Chem. Soc.* **1956**, *78*, 2380.
- (30) Zimm, B. H. *J. Chem. Phys.* **1948**, *16*, 1093, 1099.
- (31) Burchard, W.; Schmidt, M.; Stockmayer, W. H. *Macromolecules* **1980**, *13*, 1265.
- (32) Burchard, W. *Adv. Polym. Sci.* **1983**, *48*, 1.

- (33) Jones, A. A.; Brehm, G. G.; Stockmayer, W. H. *J. Polym. Sci., Polym. Sym.* 1974, No. 46, 149.
- (34) Stockmayer, W. H.; Baur, M. E. *J. Am. Chem. Soc.* 1964, 86, 3485.
- (35) Benoit, H.; Doty, P. *J. Chem. Phys.* 1953, 57, 958.
- (36) Yamakawa, H.; Fujii, M. *Macromolecules* 1973, 6, 407.
- (37) Schmidt, M.; Stockmayer, W. H. *Macromolecules*, in press.
- (38) Koyama, R. *J. Phys. Soc. Jpn.* 1973, 34, 1029.
- (39) Zugenmaier, P.; Gutknecht, W., to be published; see also: Sarko, A.; Zugenmaier, P. *ACS Symp. Ser.* 1980, No. 141, 459-482.
- (40) Yamakawa, H.; Stockmayer, W. H. *J. Chem. Phys.* 1972, 57, 2843.
- (41) Hsu, B.; McWherter, C. A.; Brant, D.; Burchard, W. *Macromolecules* 1982, 15, 1350.
- (42) We should mention here that in our recent measurements the same values for $\langle S^2 \rangle$, were found with two different instruments. Probably the lower radii determined in this work result from the improvement in the clarification of the solutions compared with the technique applied 15 years ago.
- (43) Schmidt, M.; Stockmayer, W. H.; Mansfield, M. *Macromolecules* 1982, 15, 1609.
- (44) Yamakawa, H. In "Modern Theory of Polymer Solutions"; Harper and Row: New York, 1971.
- (45) Pyun, C. W.; Fixman, M. *J. Chem. Phys.* 1964, 41, 937.
- (46) Imai, S. *J. Chem. Phys.* 1969, 50, 2116.
- (47) Yamakawa, H. *J. Chem. Phys.* 1962, 36, 2995.
- (48) Batchelor, G. K. *J. Fluid Mech.* 1972, 52, 245; 1976, 74, 1.
- (49) Felderhof, B. U. *J. Phys. A: Math. Gen.* 1978, 11, 929.
- (50) Akcasu, A. Z.; Benmouna, M. *Macromolecules* 1978, 11, 1193.
- (51) Schmidt, M. *Macromolecules*, paper submitted.
- (52) Harris, R. A.; Hearst, J. E. *J. Chem. Phys.* 1966, 44, 2595.
- (53) Hearst, J. E.; Beals, E.; Harris, R. A. *J. Chem. Phys.* 1968, 48, 537.
- (54) Zimm, B. H. *J. Chem. Phys.* 1956, 24, 269.
- (55) Scherer, P. C.; Levi, D. W.; Hawkins, M. C. *J. Polym. Sci.* 1957, 24, 19.
- (56) Gupta, A. K.; Marchal, E.; Burchard, W.; Pfannemüller, B. *J. Am. Chem. Soc.* 1979, 101, 281.
- (57) Rouse, P. E., Jr. *J. Chem. Phys.* 1953, 21, 1272.
- (58) Bueche, F. *J. Chem. Phys.* 1954, 22, 603.
- (59) Recent studies with more than two-functional primers indicate increasing difficulties for a regular enzymatic attack for steric reasons, which is observed at low primer concentration. (Ziegast, G.; Pfannemüller, B., to be published).
- (60) Sharp, P.; Bloomfield, V. A. *J. Chem. Phys.* 1968, 48, 2149.
- (61) Sharp, P.; Bloomfield, V. A. *Biopolymers* 1968, 6, 1201.
- (62) Bloomfield, V. A.; Zimm, B. H. *J. Chem. Phys.* 1966, 44, 315.

Size of Network Chains[†]

Karel Dušek

*Institute of Macromolecular Chemistry, Czechoslovak Academy of Sciences,
162 06 Prague 6, Czechoslovakia. Received July 29, 1983*

ABSTRACT: A method for calculating average degrees of polymerization and distributions of elastically active network chains (EANC), dangling chains, and EANC's with attached dangling chains is presented. The method is based on the theory of branching processes and on the Flory-Stockmayer treelike model with uncorrelated circuit closing in the gel and employs the cascade substitution and probability generating functions as a tool. The method works with the distribution of building units with respect to the number of issuing bonds having either finite or infinite continuation. The approach is developed in detail for stepwise polyaddition of f -functional components. The inadequacy in expressing the degree of polymerization of EANC's as a quantity inversely proportional to the number of EANC's for any network deviating from perfectness is stressed.

Introduction

The equilibrium elasticity of polymer networks is known to be determined by the number of elastically active network chains (EANC)¹⁻⁵ (in correlation with the effective cycle rank) and not by the degree of polymerization (size) of EANC's, provided the EANC's are sufficiently long to obey Gaussian statistics. The dangling chains are relevant only in the sense that they affect the concentration of EANC's per unit volume.

The time-dependent properties, however, are determined by the mobility of structural units of the network. They are contributed to by units in the EANC's as well as by other units present in the system—by units in the dangling chains and in the sol, if this is present. The mobility of the units in these chains is expected to depend on their average size (degree of polymerization) and possibly on the size distribution. For example, according to the Rouse theory the relaxation spectra of linear polymers depend on the weight-average degree of polymerization of the chains.⁶ There exist numerous examples that the viscoelastic properties depend on the network architecture and not only on the concentration of EANC's (cf., e.g., ref 6-8). The connection between time-dependent properties

of networks and dangling ends has been recently emphasized by Bibbó and Vallés.⁹ However, the width of the main transition region depends on the length of EANC's in a network essentially free of dangling chains; at the same time, the width and shape of the transition region of networks with the same concentration of EANC's depend on the number of dangling chains attached to EANC's.¹⁰ A theory relating the network architecture to its viscoelasticity is still missing, however.

In the literature, no united view has been forwarded on the size of network chains. Most often, the degree of polymerization or molecular weight between cross-links, M_c , is considered merely to be inversely proportional to the concentration of EANC's, and sometimes a correction for dangling chains¹¹ is applied. A rigorous method for calculating the number-average degree of polymerization has been offered by Dobson and Gordon,¹² who used the theory of branching processes employing the treelike model and cascade substitution. Recently, Bibbó and Vallés⁹ have examined the size and size distribution of dangling chains formed from monomer units with equal and independent reactivities of functional groups using the conditional probability method.

The aim of the present contribution is to present a treatment for calculating the degree of polymerization averages and distributions of both EANC's and dangling chains. The theory of branching processes developed or-

[†]Affectionately dedicated to Professor Walter H. Stockmayer, whose integrity and dedication to polymer science has long been an inspiration to the scientific community.